Supporting information

Chemical Bonding Construction of rGO-anchored Few-layer Bismuth Oxychloride for Synergistically Improving Sodium-Ion Storage

Jianguo Sun[a], Wenqiang Tu[a, e], Chao Chen[a, b], Anna Plewa[a], Hualin Ye[c], Jin An Sam Oh[a, d], Linchun He[a], Tian Wu[f *], Kaiyang Zeng[a], Li Lu[a, b *]

[a] Department of Mechanical Engineering, National University of Singapore, Singapore, 117575, Singapore

[b] National University of Singapore Suzhou Research Institute, Suzhou, 215123, China

[c] Department of Chemical & Biomolecular Engineering, National University of Singapore, Singapore, 117585, Singapore

[d] NUS Graduate School for Integrative Sciences and Engineering, National University of Singapore, Singapore, 119077, Singapore

[e] School of Chemistry and Environment, South China Normal of University, Guangzhou, 510631, China

[f] Institute of Materials Research and Engineering, Hubei University of Education, Wuhan 430205, China

[*]Corresponding Author: Li Lu (Luli@nus.edu.sg); Tian Wu (twu@whu.edu.cn)

Results and discussions

$Na_3V_2(PO_4)_3$ was synthesized via sol-gel assisted the hydrothermal process. Firstly, NH_4VO_3 was dissolved in deionized water at 80 ^{o}C, then citric acid was added into the solution with a molar ratio of 1.5:1 (Citric acid:NH_4VO_3). Citric acid acts as a chelating agent and carbon source. Subsequently, an appropriate amount of Na_2CO_3 and $NH_4H_2PO_4$ were added into the solution and stirred to obtain a homogeneous solution. Finally, the solution was transferred into Teflon lined autoclave and kept at 180 ^{o}C for 40 h. The obtained aerogel was crushed and GO was added into the mixture and stirred vigorously on a hot plate to evaporate excess water overnight. The precursor was preheated at 350 ^{o}C for 5 h in Ar atmosphere. The preheated precursor was grounded and calcined at 750 ^{o}C for 8 h in Ar/H_2 (95:5).

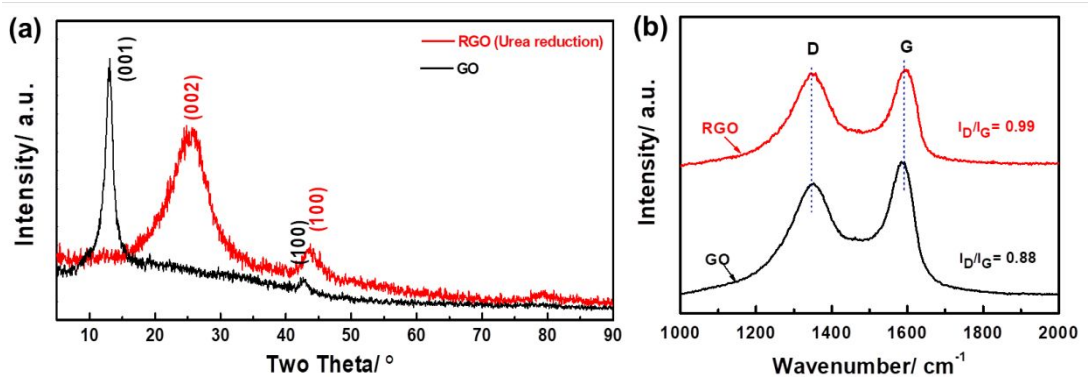

Figure S1. (a) X-ray diffraction results of GO and rGO reduced by urea, (b) the Raman spectra of GO and rGO.

In order to check the degree of reduction GO to rGO in BOC/rGO by urea, control experiment under the same condition was performed. as shown in Figure S1, The peak at 2θ = 12.1° dues to (001) plane for GO, In contrast, the major diffraction peak (002) appears at 25.2°, which is induced by the reduced interlayer distance by the reduction of oxygenated functional groups between the carbon layers[1]. Furthermore, the intensity of the peak ratio I_D/I_G exhibits an obvious increment from 0.88 to 0.99, which can be attributed to the increased sp^2 carbon atoms and defects in the matrix by reduction[2]. This further indicates that GO has been partly reduced to rGO.

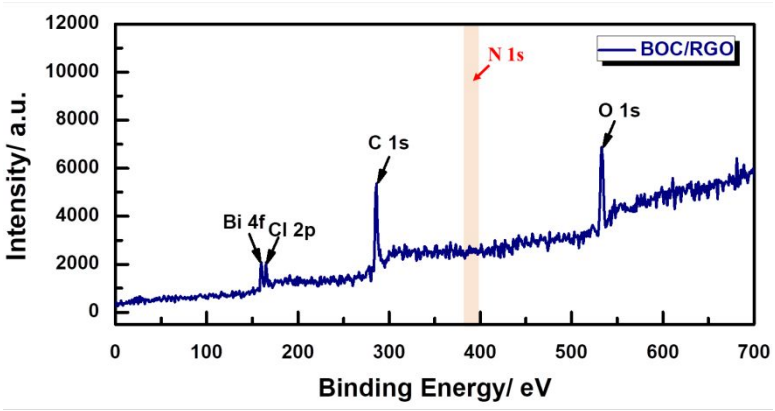

Figure S2. The XPS full spectra of BOC/rGO sample.

As shown in Figure S2, the full XPS spectra show typical XPS peaks for Bi*4f*, Cl*2p*, C*1s* and O*1s*, which is in line with the chemical composition of BOC/rGO. It is obvious that there is no N*1s* XPS peak in the range of 380-400 eV, demonstrating no nitrogen atoms were induced into rGO by urea reduction.

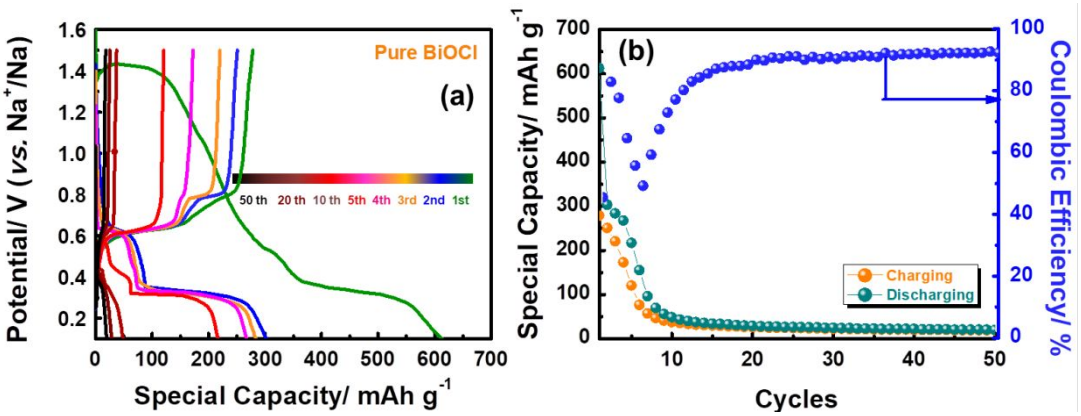

Figure S3. (a) The charge/discharge curves of the pure BiOCl and (b) cycling performance and coulombic efficiency of the pure BiOCl.

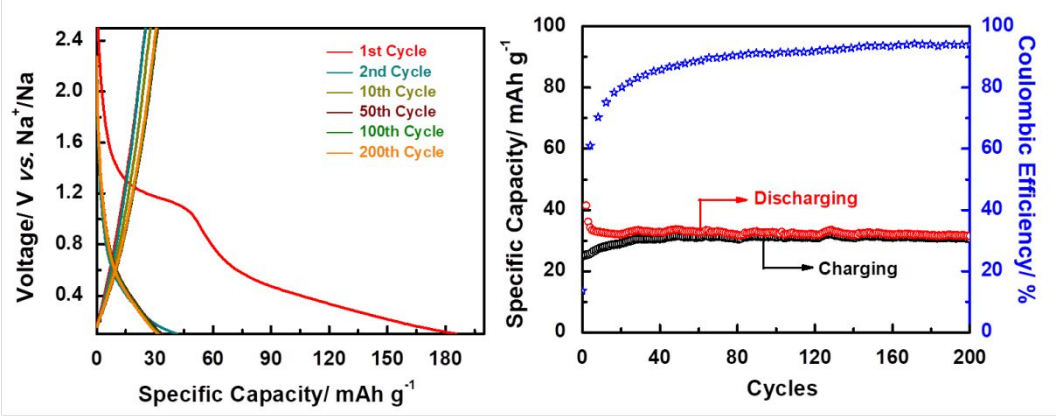

Figure S4. (a) The charge/discharge curves of the pure rGO and (b) Cycling performance and coulombic efficiency of the pure rGO.

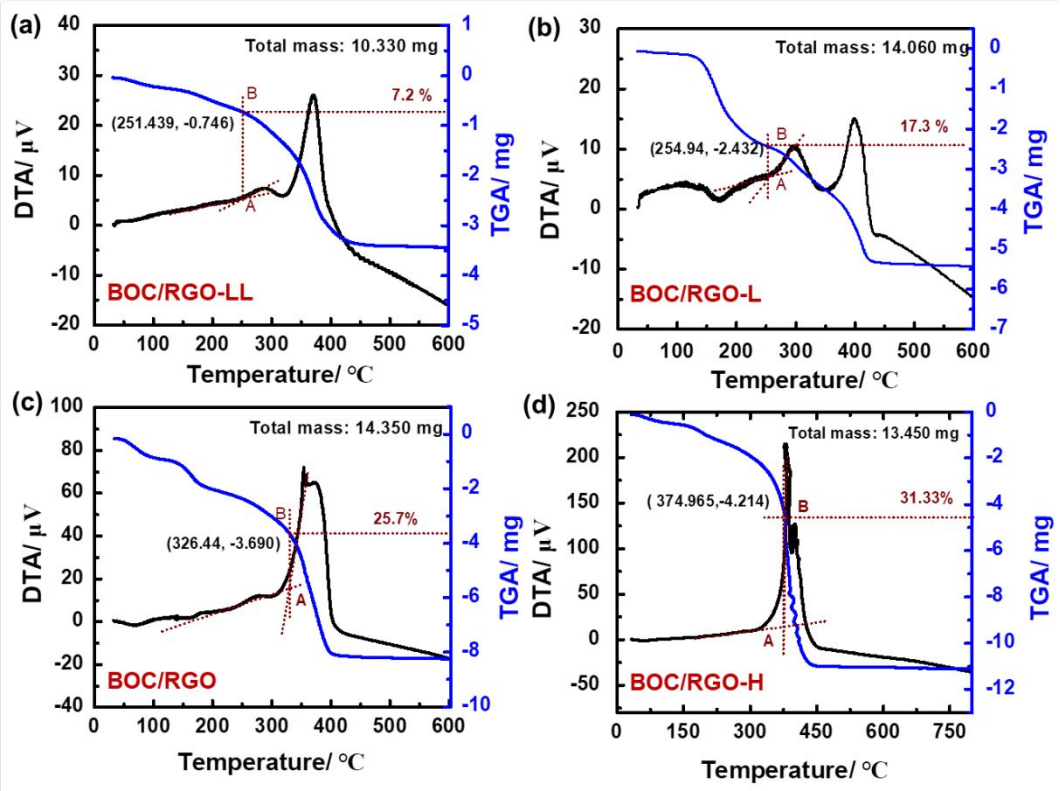

Figure S5. (a-d) The BOC/RGO at different amount of rGO from 7.2%, 17.3%, 25.7%, 31.33%, named as BOC/RGO-LL, BOC-RGO-L, BOC-RGO, BOC-RGO-H.

Thermogravimetric analysis was carried out using a SHIMADZU Differential Thermal-Thermogravimetric Analyzers (SHIMADZU, DTG-60H from room temperature to 1000 ℃ at a scan rate of 5 ℃/min under oxygen protection. As shown in Figure S5, a typical endothermic peak appeared at about 300-350 ℃, which can be assigned to the decomposition of BiOCl. After calibration, the obtained results showed the rGO amount of BOC/RGO-LL, BOC-RGO-L, BOC-RGO, BOC-RGO-H is 7.2%, 17.3%, 25.7%, and 31.33%, respectively.

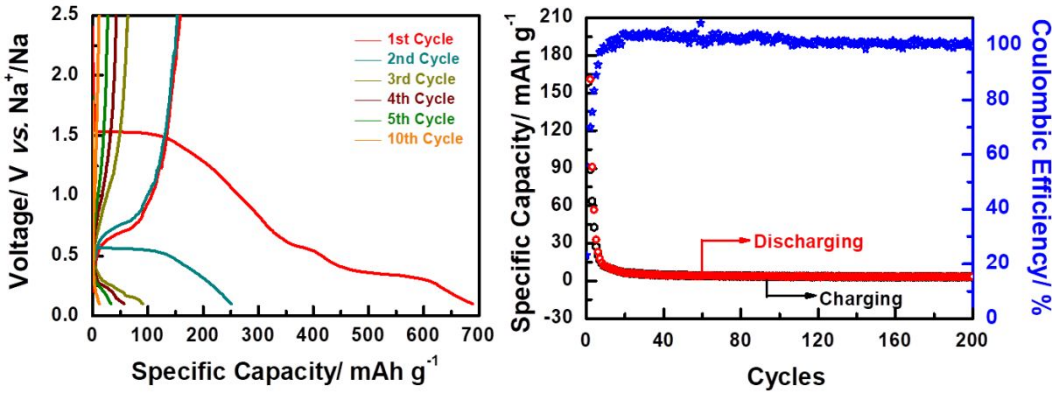

Figure S6. (a) The charge/discharge curves of BiOCl@rGO and (b) cycle performance and columbic efficiency of BiOCl@rGO.

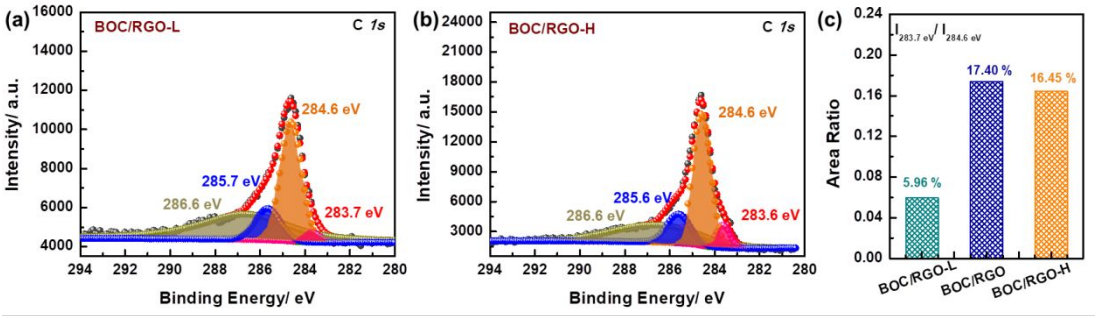

Figure S7. (a-b) XPS spectra of C *1s* for BOC/RGO-L and BOC/RGO-H. (c) the area ration of peak 283.7 eV vs. peak 284.6 eV.

In order to evaluate the amounts of Bi-C bonds on improving the electrochemical properties, XPS spectra were further performed to estimate the amounts of Bi-C bonding. As shown in Figure S7, similar peaks were observed in the C*1s* XPS spectra of BOC/RGO-L and BOC/RGO-H, the peak at 284.6 eV can be assigned to the -C-C bands, while the other two peaks located at 285.6(7) eV and 286.6 eV can be assigned to -C-H and -C-O-C (or -C-OH) bands, respectively. Besides, a small peak located at 283.6(7) eV can be assigned to the Bi-C bonds, in line with the observation of lower chemical valance of bismuth. At the same time, the intensity ratio between peak (284.6 eV) and peak (283.6(7) eV) is 5.64%, 17.4%, and 16.45% for BOC/RGO-L, BOC/RGO, and BOC/RGO-H respectively, indicating the amount of Bi-C bonds increases upon rGO mass and reaches an optimized value of around 17%. However, it is worthy noticed that even though the amount of interfacial Bi-C bonds of BOC/RGO-H is quite similar to that of BOC/RGO, the specific capacity of BOC/RGO-H is much lower, the lower capacity may be caused by the longer Na^+ diffusion path length and the higher migration energy barrier induced by randomly stacked excess rGO. It further confirms that the excellent electrochemical properties of BOC/RGO are attributed to the synergistic effect of the interfacial Bi-C bonding coupling and effective rGO wrapping instead of the independent effect.

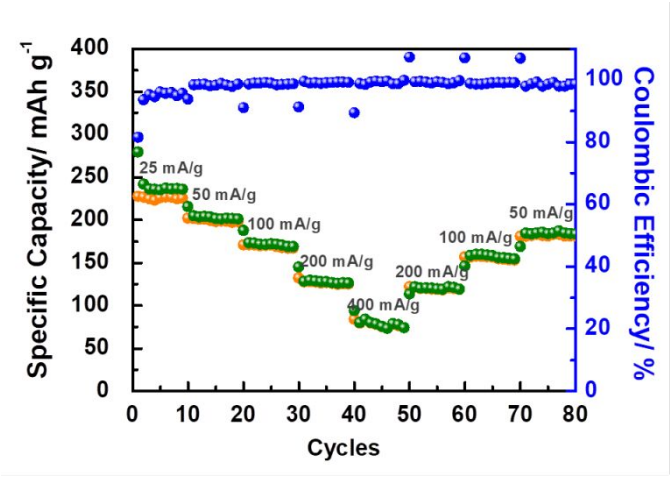

Figure S8. Rate performance of the BOC/rGO anode for SIBs

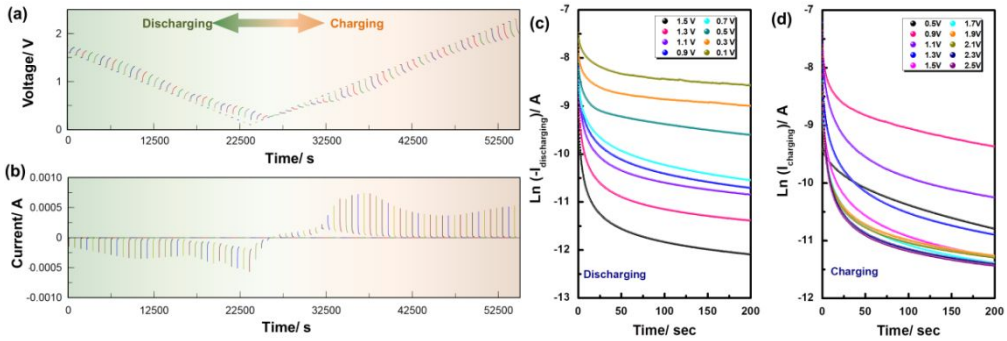

Figure S9. (a-b) The voltage and current change with time during PITT performance for BOC/rGO, and (c-d) the current decays with time for discharge and charge process.

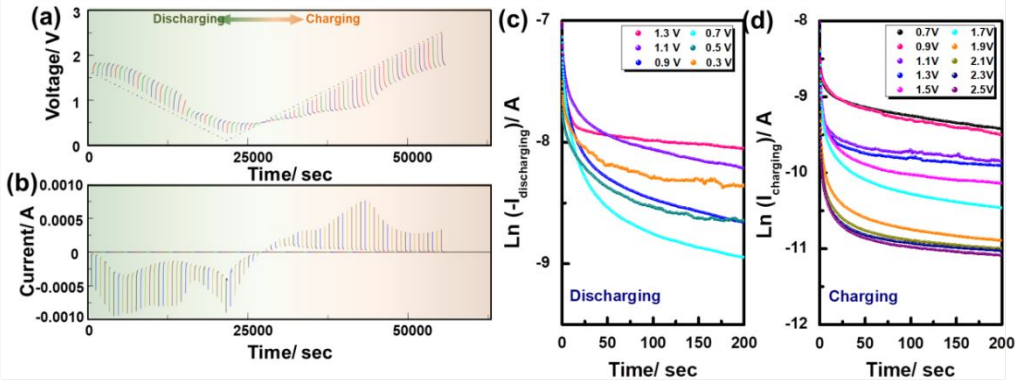

Figure S10. (a-b) The voltage and current change with time during PITT performance for BOC@rGO, and (c-d) the current decays with time for discharge and charge process.

The potentiostatic intermittent titration technique (PITT) was performed with a potential step of 200 mV was applied from open voltage to 2.5 V, at each step, the voltage was kept for 200 s and the current was recorded as a function of time, after that, the potential was removed and relaxed for 500 s before next potential. (Figure

S10). the time (t) dependence of the transient current (I_t) at each potential voltage can be expressed by the following equation[3]:

$$I_t = \frac{2FS(C_S - C_0)D_{Na}}{L}\exp\left(\frac{\pi^2 D_{Na} t}{4L^2}\right) \quad (1)$$

$$D_{Na} = -\frac{dln(I_t)4L^2}{dt\ \ \pi^2} \quad (2)$$

where S the surface area of the electrode, F is the Faraday constant, C_s-C_0 is the concentration difference at the surface and L the thickness of electrode materials. After plotting Ln(I_t) *vs.* t, we can get the sodium diffusion coefficient from Eq. (2).

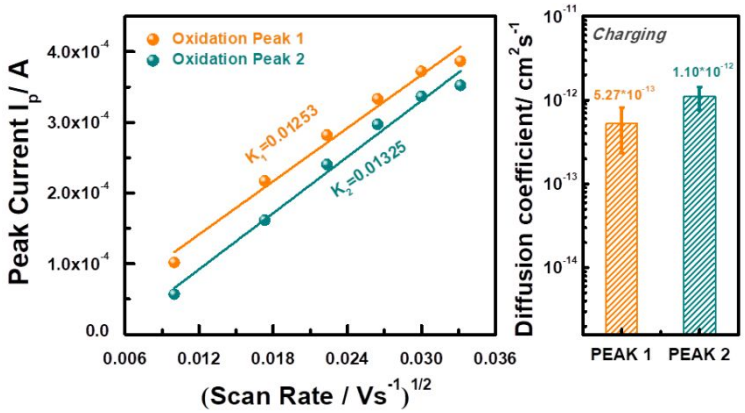

Figure S11. (a) The two oxidation peak current vs. scan rate (Vs^{-1}) and (b) the calculated diffusion coefficient from two oxidation peaks.

Figure S11 shows the peak current I_p vs. square root of the sweeping rate from 0.1-3.0 mVs^{-1} in the voltage range of 0.1-2.5 V vs Na^+/Na, which has been recorded by the CV spectra of BOC/rGO from Figure 4a. In the case of the semi-infinite and finite diffusion, the peak current I_p is proportional to the square root of the sweeping rate ($v^{1/2}$) for any separated redox reaction in CV curve, which can be expressed as follow[4, 5]:

$$I_p = 2.69\times10^5\, n^{3/2}\, AD^{1/2}\, v^{1/2}\, \Delta C_o \quad (3)$$

where n is the number of electrons transferred in reaction, A is the area of the electrode, D is the diffusion coefficient, ΔC_o is the change in concentration corresponding to the specific electrochemical reaction, which is estimated by the change of the quantity of electric charge by the integral area of peak in our experiment[6]. The calculated D value order is in line with the results calculated from PITT testing as shown in Figure 5 (a).

References

(1) Liu, G.; Wang, L.; Wang, B.; Gao, T.; Wang, D., A reduced graphene oxide modified metallic cobalt composite with superior electrochemical performance for supercapacitors. *Rsc Adv.* **2015,** *5*, 63553-63560.

(2) Ramakrishnan, K.; Nithya, C.; Kundoly Purushothaman, B.; Kumar, N.; Gopukumar, S., Sb_2O_4@ rGO Nanocomposite Anode for High Performance Sodium-Ion Batteries. *ACS Sustainable Chem. Eng.* **2017,** *5*, 5090-5098.

(3) Xie, J.; Tanaka, T.; Imanishi, N.; Matsumura, T.; Hirano, A.; Takeda, Y.; Yamamoto, O., Li-ion transport kinetics in $LiMn_2O_4$ thin films prepared by radio frequency magnetron sputtering. *J Power Sources* **2008,** *180*, 576-581.

(4) Levi, M. D.; Aurbach, D., The mechanism of lithium intercalation in graphite film electrodes in aprotic media. Part 1. High resolution slow scan rate cyclic voltammetric studies and modeling. *J ELECTROANAL CHEM* **1997,** *421*, 79-88.

(5) Bard, A. J.; Faulkner, L. R.; Leddy, J.; Zoski, C. G., *Electrochemical methods: fundamentals and applications*. wiley New York: 1980; Vol. 2.

(6) Das, S.; Majumder, S.; Katiyar, R., Kinetic analysis of the Li+ ion intercalation behavior of solution derived nano-crystalline lithium manganate thin films. *J Power Sources* **2005,** *139*, 261-268.